Impact of Human Blockage on 5G Communication System in the 26 GHz Band

Hamidou Dembele, Marie Le Bot, Francois Gallee, Patrice Pajusco

Impact of Human Blockage on 5G Communication System in the 26 GHz Band

Hamidou DEMBELE*†, Marie LE BOT*, François GALLEE†, Patrice PAJUSCO†
*Orange Labs, Cesson-Sévigné, France, hamidou.dembele@orange.com
†Dpt. Microwaves, IMT-Atlantique, Brest, France

***Abstract*—This paper deals with the impact of human blockage on 5G communication systems in millimeter-wave bands. The analysis of communication performance in terms of block error rate with and without the influence of human blockage is proposed in the 26 GHz band, thanks to the implementation of the 5G physical layer in a simulation tool. Based on the block error rate performance, a link budget is also established in order to evaluate the impact of blockage on the cell coverage.**

***Index Terms*—Human blockage, mmWaves, 26 GHz, propagation, 5G, BLER, link budget, antenna.**

I. Introduction

The 5G New Radio (NR) is standardized by the 3rd Generation Partnership Project (3GPP) with several changes in the physical (PHY) layer processing. Regarding the channel, a 3D model based on clustered delay line (CDL) is designed including antenna radiation pattern defined in elevation and azimuth for the link-level evaluations. This channel model is proposed for carrier frequencies extended to millimeter wave (mmWave) bands up to 100 GHz.

The NR communication chain at the transmitter is proposed for diversifying 5G major use-cases, among which the enhanced mobile broadband (eMBB) applications, that requires high data rates. In this context, the use of mmWave bands takes advantage of the enormous amount of spectrum available in this region of frequencies.

Although these frequencies offer opportunities in terms of huge bandwidth for wireless communication, they are victims of severe attenuation with high sensitivity to blockage leading to communication failure due to the presence of human or vehicle in the propagation environment.

In the literature, several theoretical and experimental approaches are proposed for modelling human blockage in mmWave bands for 5G communication. Nonetheless, the consequence of the attenuation due to the presence of human or vehicle on the 5G communication system is rarely investigated. In [2], Momo and Mowla analyse the impact of human blockage on the channel statistics such as root mean square (RMS) delay spread and pathloss in the 28, 38, 60 and 73 GHz bands. Moltchanov *et al.* [3] justify that the presence of human blockers between the user and the base station (BS) leads a serious drop in the throughput at the 5G NR air interface at 28 GHz. To our knowledge, so far there are no works reported in the open literature on the impact of human attenuation on the end-to-end 5G PHY layer communication performance in terms of block error rate (BLER).

The first objective of this paper is to evaluate the BLER performance of the entire 5G physical layer chain in the 26 GHz mmWave band using sector antenna. And then the influence of human blockage on these results is highlighted. The second objective is to establish from the resulting BLER, the link budget for the cell coverage with and without blockage.

The rest of the paper is organized as follows. Section II briefly describes the 5G NR communication system in downlink. In section III, the propagation channel model used in this work is presented. Section IV focuses on the model of human blockage implemented in the communication chain. Section V is dedicated to simulation results. And finally, conclusion and future studies are given in section VI.

II. 5G Communication System Model

The goal of this section is to give an overview of the 5G downlink transmission chain implemented as part of this study. The end-to-end data processing is highlighted in Fig. 1, including both transmitter and receiver chains.

A. 5G PHY Transmission Chain

Several processing blocks are defined in the 3GPP specification [4] and [5] for the 5G NR data transmission. Fig. 1 shows that after the generation of a transport block, a sequence of cyclic redundancy check (CRC) bits is computed and attached to this one before low-density parity check (LDPC) channel encoding and the rate matching processing. The goal of the rate matching block in the communication chain is to dynamically adapt the number of bits on LDPC encoder output to the amount of bits expected for a given modulation and coding scheme (MCS). Multiple-input multiple-output (MIMO) precoding is applied here in order to adapt the number of spatial layers (streams) to the number of antennas active for the transmission. Before the transmission of data, orthogonal frequency-division multiplex (OFDM) numerology is used.

B. PHY Processing at the Receiver

After receiving data symbols, the first key signal processing here is the equalization operation whose purpose is to compensate different distortions or fading incurred by the signal through the transmission channel. In this communication chain, minimum mean square error (MMSE) equalizer is implemented. Furthermore, another key processing is the soft demodulation used to convert the equalized data symbols to a stream of values needed for LDPC decoding algorithms.

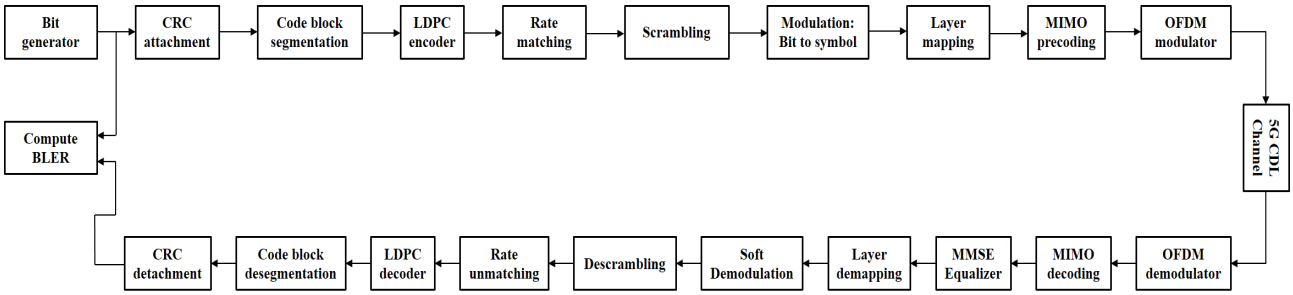

Fig. 1: Communication block diagram of 5G NR.

Decoded bits from LDPC decoder are delivered for BLER computation after code block desegmentation and CRC detachment which represent the reverse functionalities of code block segmentation and CRC attachment at the transmitter, respectively. To determine the performance of the entire communication chain, the BLER is calculated by comparing the initial transport block with that received.

III. CDL Channel Model

For the multipath propagation model regarding the communication system, clustered delay line (CDL) channel models in [6] are adopted. CDL models were designed for 3D propagation characterized by departure and arrival angles in elevation and azimuth as illustrated in Fig. 2 with $\phi_{n,m,AoD}$, $\theta_{n,m,ZoD}$, $\phi_{n,m,AoA}$ and $\theta_{n,m,ZoA}$ representing azimuth angle of departure, elevation angle of departure, azimuth angle of arrival and elevation angle of arrival of ray m within cluster n, respectively.

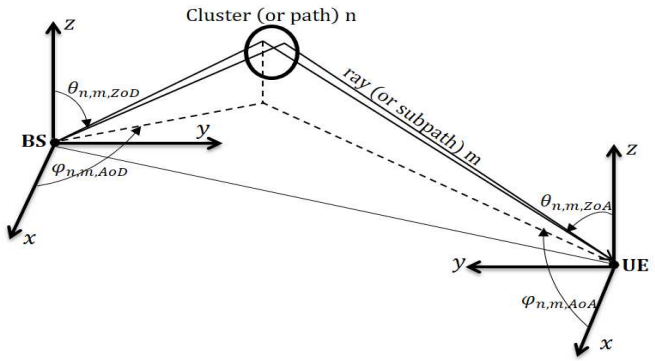

Fig. 2: Clustered multipath propagation.

Their expressions are defined hereby [6]:

$$\phi_{n,m,AoD} = \phi_{n,AoD} + c_{ASD}\alpha_m, \quad (1)$$

$$\phi_{n,m,AoA} = \phi_{n,AoA} + c_{ASA}\alpha_m, \quad (2)$$

$$\theta_{n,m,ZoD} = \theta_{n,ZoD} + c_{ZSD}\alpha_m, \quad (3)$$

$$\theta_{n,m,ZoA} = \theta_{n,ZoA} + c_{ZSA}\alpha_m, \quad (4)$$

where c_{ASD}, c_{ASA}, c_{ZSD} and c_{ZSA} represent azimuth spread of departure angle, azimuth spread of arrival angle, elevation spread of departure angle and elevation spread of arrival angle, respectively, for the selected profile. $\phi_{n,AoD}$, $\theta_{n,ZoD}$, $\phi_{n,AoA}$ and $\theta_{n,ZoA}$ are azimuth angle of departure, elevation angle of departure, azimuth angle of arrival and elevation angle of arrival of cluster n, respectively. α_m defines the offset of ray m angle within the cluster whose values are given in the specification.

TABLE I: CDL E profile parameters.

Cluster n	Normalized delay $\tau_{n,model}$	Power [dB] P_n	AoD [°] $\varphi_{n,AoD}$	AoA [°] $\varphi_{n,AoA}$	ZoD [°] $\theta_{n,ZoD}$	ZoA [°] $\theta_{n,ZoA}$
1	0.000	−0.03	0	−180	99.6	80.4
	0.000	−22.03	0	−180	99.6	80.4
2	0.5133	−15.8	57.5	18.2	104.2	80.4
3	0.5440	−18.1	57.5	18.2	104.2	80.4
4	0.5440	−22.9	−20.1	101.8	99.4	80.8
5	0.5630	−19.8	57.5	18.2	104.2	80.4
6	0.7112	−22.4	16.2	112.9	100.8	86.3
7	1.9092	−18.6	9.3	−155.5	98.8	82.7
8	1.9293	−20.8	9.3	−155.5	98.8	82.7
9	1.9589	−22.6	9.3	−155.5	98.8	82.7
10	2.6426	−22.3	19	−143.3	100.8	82.9
11	3.7136	−25.6	32.7	−94.7	96.4	88
12	5.4524	−20.2	0.5	147	98.9	81
13	12.0034	−29.8	55.9	−36.2	95.6	88.6
14	20.6419	−29.2	57.6	−26	104.6	78.3

Per − Cluster Parameters				
Parameter	C_{ASD}	C_{ASA}	C_{ZSD}	C_{ZSA}
Value	5°	11°	3°	7°

Five different CDL profiles are proposed as follow. Three profiles for non-line of sight (NLOS) state propagation which are CDL A, CDL B and CDL C. For line of sight (LOS) environment, two profiles CDL D and CDL E are used. Table I summarizes CDL E profile parameters used as channel model in the context of this study. In CDL channel model, the principle of delay scaling factor $DS_{desired}$ is introduced from which the propagation delay τ_n of cluster n is defined by:

$$\tau_n = \tau_{n,model} \cdot DS_{desired}, \quad (5)$$

with $\tau_{n,model}$ the normalized delay of cluster n whose values are mentioned for each CDL profile, namely CDL E.

IV. 3GPP Blockage Model

As mentioned in the introduction of the paper, realistic experimental results have been published in the literature on human attenuation values in mmWave bands. Some models are based on the diffraction theory from which a computational formula is derived to predict the blockage attenuation. However, in this work about the 5G communication, we mainly focused on the modelling standardized by the 3GPP.

A. General Description

Blockage constitutes one of mmWave propagation channel features, which is characterized by severe attenuation of signal strength caused by pedestrians or vehicles. Two types of blockages are identified, one is called *self-blocking*, which means that the radio link is blocked by the user itself most often by its hand. The other type called *non-self-blocking* is due to the presence of humans or vehicles moving around the user. Both types are presented in Fig. 3.

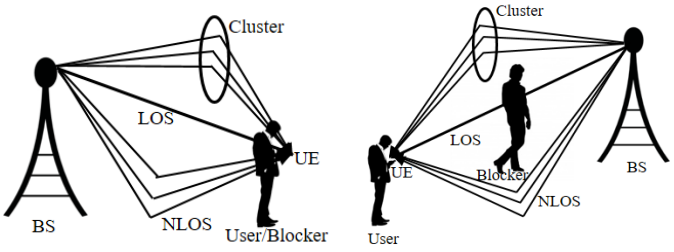

(a) Self-blocking (b) Non-self-blocking

Fig. 3: Blocking scenario.

Note that the presence of blockers in this context of study does not change the channel state, i.e the LOS state cannot change in NLOS even if the direct path is blocked. The idea of blocking a cluster is just to attenuate the channel gain of this cluster as detailed in the rest of the section.

B. Blockage Modelling

In the 3GPP specification, two models (A and B) of blockage are proposed, each with a specific use case. Model A is used in computational environment and model B is desired when a realistic environment is adopted. In our study, we only focused on the approach given in model A. As illustrated in Fig. 4, model A is a stochastic model in which the blocker is modelled by a blocking region at the receiver. The principle

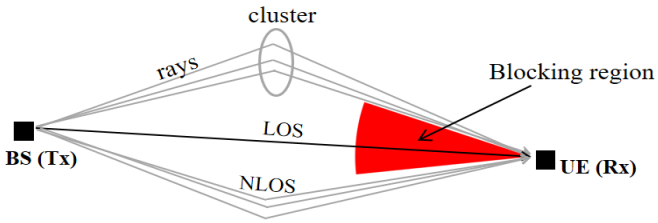

Fig. 4: Blocking scenario.

of this approach is to attenuate any cluster whose arrival angle falls into the blocking region. The blocking region is characterized by an angular spread in elevation defined from $\theta_c - \Delta\theta$ to $\theta_c + \Delta\theta$ and an angular spread in azimuth defined from $\phi_c - \Delta\phi$ to $\phi_c + \Delta\phi$. $\Delta\theta$ and $\Delta\phi$ represent angular spread with high attenuation centred around θ_c and ϕ_c in elevation and azimuth, respectively. It is clear that a cluster is blocked if its arrival angles in elevation θ_{ZoA} and azimuth ϕ_{AoA} are such that $\theta_{ZoA} \in \{\theta_c - \Delta\theta, \theta_c + \Delta\theta\}$ and $\phi_{AoA} \in \{\phi_c - \Delta\phi, \phi_c + \Delta\phi\}$, and the channel gain associated to this cluster is attenuated in dB units by [6]:

$$L_{dB} = -20\log_{10}\left(1 - \left(F\left(a_1\right) + F\left(a_2\right)\right) \cdot \left(F\left(z_1\right) + F\left(z_2\right)\right)\right), \tag{6}$$

where $a_1 = \phi_{AoA} - \left(\phi_c + \frac{\Delta\phi}{2}\right)$, $a_2 = \phi_{AoA} - \left(\phi_c - \frac{\Delta\phi}{2}\right)$, $z_1 = \theta_{AoA} - \left(\theta_c + \frac{\Delta\theta}{2}\right)$ and $z_2 = \theta_{AoA} - \left(\theta_c - \frac{\Delta\theta}{2}\right)$ and $F\left(x\right)$ is defined for $x \in \{a_1, a_2, z_1, z_2\}$ by:

$$F\left(x\right) = s\left(x\right)\frac{1}{\pi}atan\left(\frac{\pi}{2}\sqrt{\frac{\pi}{\lambda_0}r\left(\frac{1}{cos\left(x\right)} - 1\right)}\right), \tag{7}$$

with

$$s\left(x\right) = \begin{cases} +1 & \text{if } x \leq 0 \\ -1 & \text{if } x > 0 \end{cases}, x \in \{a_1, z_1\}, \tag{8}$$

or

$$s\left(x\right) = \begin{cases} +1 & \text{if } x > 0 \\ -1 & \text{if } x \leq 0 \end{cases}, x \in \{a_2, z_2\}. \tag{9}$$

And r in (7) represents the distance from the blocker to the receiver (Rx).

V. Simulation Results

This section is dedicated to the presentation and analysis of simulation results regarding the scenarios of interest as well as the study assumptions. The whole 5G physical layer including the multipath channel with the blockage phenomenon, has been developed in C++ based simulation tool. Only one base station (BS) considered as the transmitter and one user equipment (UE) considered as the receiver are used. The communication chain given in Fig. 1 is used for link-level evaluation. Both scenarios with and without human blockage are considered in indoor environment. The blocking system is applied such that the LOS path fully meets the center of the blocker whose parameters are given in Table II. We assume that the blockage phenomenon occurs during the whole data transmission between the BS and the UE. The same antenna model is used for transmission and reception, and its boresight almost matches the LOS path of the CDL E profile.

TABLE II: Simulation Parameters.

Parameters	Values
Carrier frequency	26 GHz
Bandwidth	400 MHz [15]
Sub-carrier spacing	120 kHz [15]
FFT size	4096
Channel model	3GPP LOS Channel Profile CDL E, $DS_{desired} = 100\,ns$ [6]
Blocking region parameters	$\Delta\phi = 45°$, $\phi_c = -180°$, $\Delta\theta = 15°$, $\theta_c = 80.4°$, $r = 2\,m$
Number of human blockers	1
Channel estimation	Ideal
Antenna model	3GPP sector antenna radiation pattern with gain $G_{max} = 8$ dBi [6]
LDPC decoding algorithm	Normalized Min-Sum (NMS) with normalization factor $\alpha = 0.7$
LDPC decoding iterations	50

A. Attenuation from human blockage at 26 GHz

We first start by analyzing the attenuation by human body in the 26 GHz band using the 3GPP blockage model presented in section IV-B.

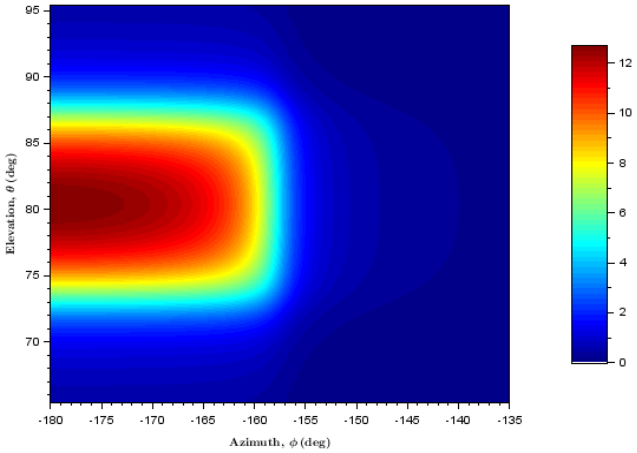

Fig. 5: Human blockage attenuation in dB units.

Fig. 5 shows this attenuation in dB units with respect to azimuth ϕ and elevation θ angles in the blocking region with parameters given in Table II. From this figure, we notice that the attenuation is all the more significant as the direction of propagation path or cluster is closer to the center of the blocker characterized here by angle in azimuth $\phi_c = -180°$ and angle in elevation $\theta_c = 80.4°$. This mechanism is justified by the modelling of human blocker through a rectangular screen for which a diffraction loss given in (7) is applied. The diffraction approach highlights the fact that if the cluster is closer to the knife-edges of the screen, the signal power is very lowly attenuated. And if the cluster meets the center of the screen, the signal strength is attenuated to the maximum. Note that due to cosine expression in (7), the value of attenuation admits a symmetric axis in each of both plans, azimuth and elevation through ϕ_c and θ_c, respectively. Therefore, the attenuation ranges from 0 to 12.71 dB at 26 GHz for one blocker. These theoretical values are justified by measurements conducted by Zhao *et al.* [7] in indoor environment to quantify the value of human body attenuation at 26 GHz. Results show that the communication link is attenuated by a maximum value of 12.66 dB for the presence of one person between the Tx and the Rx.
Nonetheless, it is obvious that if the number of human blockers increases, the resulting attenuation also increases.

B. Link Level Evaluation

The actual 5G NR is performed here in order to show that the impact of human blockage can be observed on communication performance in terms of BLER. For the link level evaluation, a single-input single output (SISO) scenario is chosen. As previously mentioned, the advantage of mmWave is

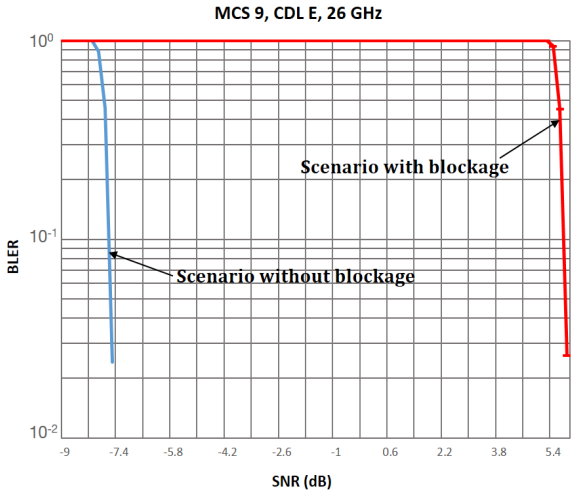

Fig. 6: BLER vs SNR in SISO.

TABLE III: Link Budget in 26 GHz band.

Parameter	Scenario without blockage	Scenario with blockage
TX power	10 dBm	10 dBm
TX antenna gain	8 dBi	8 dBi
TX cable loss	3 dB	3 dB
EIRP	**15 dBm**	**15 dBm**
Thermal noise density	-174 dBm/Hz	-174 dBm/Hz
Noise bandwidth (400 MHz)	85.8 dB	85.8 dB
RX noise figure	9 dB	9 dB
Thermal noise	-79.20 dBm	-79.20 dBm
Noise rise	3 dB	3 dB
RX antenna gain	8 dBi	8 dBi
RX cable loss	0 dB	0 dB
Required SNR for BLER=10%	-7.7 dB	5.7 dB
Rx sensitivity	**-91.90 dBm**	**-78.50 dBm**
Cell coverage probability	95%	95%
Shadowing standard deviation	3 dB	3 dB
Shadow margin	**2.95 dB**	**2.95 dB**
Path loss max PL_{max}	**103.95 dB**	**95.55 dB**

focused on 5G eMBB applications for which the target BLER is 10% [8]. Fig. 6 highlights the BLER vs SNR performance for both scenarios with and without blockage using MCS 9 (16QAM, code rate = 0.6) and CDL E channel model with one antenna at the transmitter and one antenna at the receiver. The shape of the curves is typical of scenarios with LDPC channel coding. For BLER=10%, we observe that the link without blocker is better than the link including human blocker with a signal-to-noise ratio (SNR) difference about 13 dB. This result is justified by the blockage (attenuation of 12.71 dB) of the LOS path which is the most dominant path. The same trend is observed by comparing the channel power of CDL E profile without blockage with this one of CDL E including the blockage of the LOS cluster.

From the performance BLER=10% given in Fig. 6, we establish the link budget in order to illustrate the consequence of human blockage phenomenon on the system capacity in terms of cell coverage in mobile communication as given in Table III. To this end, PL_{max} represents the maximum value of path loss to determine the cell range in both scenarios with and without the presence of human blockage on the communication link. In the calculation, we consider a transmit

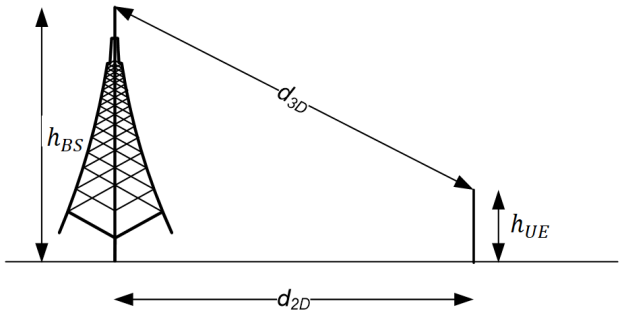

Fig. 7: Illustration of d_{3D}, d_{2D}, h_{BS} and h_{UE}.

power of 10 dBm [11] and a coverage probability of 95%.

Based on this cell coverage probability and by assuming that Gaussian shadowing is considered with standard deviation of 3 dB, a shadowing margin of 2.95 dB is deduced.
As defined in [6], the path loss in LOS state propagation environment is defined by:

$$PL_{LOS}\,(dB) = 32.4 + 17.3\log_{10}\left(d_{3D}\right) + 20\log_{10}\left(f_c\right), \quad (10)$$

where $d_{3D} = \sqrt{d_{2D}^2 + \left(h_{BS} - h_{UE}\right)^2}$, with d_{2D} the distance from the BS to the UE which defines the cell range, h_{BS} and h_{UE} the BS and UE heights, respectively, and f_c is the carrier frequency. With the maximum path loss PL_{max} from the link budget, for $h_{BS} = 3m$ and $h_{UE} = 1.5m$ in the 26 GHz band, we deduce from (10) that the scenario without human presence on the LOS link has a cell range of $d_{2D_{max}} = 316.3\ m$ while the blockage of the LOS link results in a cell range of $d_{2D_{max}} = 53.13\ m$. From this analysis, it can be seen that to guarantee the same quality of service, the communication range must be drastically reduced in the 26 GHz mmWave band.

VI. Conclusion

In this paper, the problem of human blockage that occurs in 26 GHz band for 5G communication system is addressed. To this end, we analyzed in a simulation tool the 5G physical layer, the multipath channel and the blockage model. Simulation results revealed that for the same 5G eMBB quality of service, the 26 GHz communication system with the presence of human in the LOS cluster requires a 13 dB increase in SNR compared to the similar scenario without blockage. For future work, we will extend the analysis to antenna pattern diversity in the context of multi-antenna systems as resolution of communication link blockage by a human.

References

[1] Y. Niu, Y. Li, D. Jin, L. Su and A. V. Vasilakos,"A survey of millimeter wave communications (mmWave) for 5G: opportunities and challenges," Springer Wireless Networks, pp. :2657–2676, February 2015.

[2] S. H. A. Momo and M. M. Mowla, "Effect of Human Blockage on an Outdoor mmWave Channel for 5G Communication Networks," in *2019 22nd International Conference on Computer and Information Technology (ICCIT)*. Dhaka, Bangladesh, Bangladesh: IEEE, December 2019.

[3] D. Moltchanov, A. Ometov, P. Kustarev, O. Evsutin, J. Hosek and Y. Koucheryavy, "Analytical TCP Model for Millimeter-Wave 5G NR Systems in Dynamic Human Body Blockage Environment," Sensors, July 2020.

[4] 3GPP, "Technical Specification Group Radio Access Network; NR; Multiplexing and channel coding," Tech. Rep., September 2018, 3GPP TS 38.212 V15.3.0.

[5] 3GPP, "Technical Specification Group Radio Access Network; NR; Physical channels and modulation," Tech. Rep., September 2018, 3GPP TS 38.211 V15.3.0.

[6] 3GPP, "Technical Specification Group Radio Access Network; Study on channel model for frequencies from 0.5 to 100 GHz," Tech. Rep., June 2018, 3GPP TS 38.901 V15.0.0.

[7] X. Zhao, Q. Wang, S. Li, S. Geng, M. Wang, S. Sun, and Z. Wen,"Attenuation by Human Bodies at 26- and 39.5-GHz Millimeter Wavebands," IEEE Antennas and Wireless Propagation Letters, vol. 16, pp. 1229-1232, November 2016.

[8] E. Chu, J. Yoon and B. C. Jung,"A Novel Link-to-System Mapping Technique Based on Machine Learning for 5G/IoT Wireless Networks," Sensors, March 2019.

[9] G. Barb and M. Otesteanu, "On the Influence of Delay Spread in TDL and CDL Channel Models for Downlink 5G MIMO Systems," in *2019 IEEE 10th Annual Ubiquitous Computing, Electronics and Mobile Communication Conference (UEMCON)*. New York City, NY, USA: IEEE, October 2019.

[10] Q. U. A. Nadeem, A. Kammoun and M. S. Alouini, "Elevation Beamforming with Full Dimension MIMO Architectures in 5G Systems: A Tutorial," Arxiv. Available: https://arxiv.org/pdf/1805.00225.pdf, June 2019.

[11] Y. Yu, P. G. M. Baltus, and A. H. M. van Roermund, "Phased Arrays and Architecture Selection," Analog Circuits and Signal Processing, vol 1. Springer.

[12] S. Collonge, G. Zaharia and G.E. Zein,"Influence of the human activity on wide-band characteristics of the 60 GHz indoor radio channel," IEEE Transactions on Wireless Communications, vol. 3, no. 6, pp. 2396-2406, November 2014.

[13] T. Bai and R. W. J. Heath, "Analysis of self-body blocking effects in millimeter wave cellular networks," in *48th Asilomar Conference on Signals, Systems and Computers*. Pacific Grove, CA, USA: IEEE, November 2014.

[14] 3GPP, "Technical Specification Group Radio Access Network; NR; Physical layer procedures for data," Tech. Rep., June 2019, 3GPP TS 38.214 V15.6.0.

[15] 3GPP, "Technical Specification Group Radio Access Network; NR; Base Station (BS) radio transmission and reception," Tech. Rep., September 2018, 3GPP TS 38.214 V15.3.0.

[16] Jacob *et al.*, "A ray tracing based stochastic human blockage model for the IEEE 802.11ad 60 GHz channel model," in Proceedings of the 5th European Conference on Antennas and Propagation (EUCAP). Rome, Italy: IEEE, April 2011